



Contents lists available at SciVerse ScienceDirect

Gene

journal homepage: www.elsevier.com/locate/gene

Characterization of the defense transcriptome responsive to *Fusarium oxysporum*-infection in *Arabidopsis* using RNA-seq

Qian-Hao Zhu ^{a,*}, Stuart Stephen ^a, Kemal Kazan ^b, Gulei Jin ^c, Longjiang Fan ^c, Jennifer Taylor ^a, Elizabeth S. Dennis ^a, Chris A. Helliwell ^a, Ming-Bo Wang ^{a,*}

^a CSIRO Plant Industry, Clunies Ross Road, Canberra, ACT 2601, Australia

^b CSIRO Plant Industry, 306 Carmody Road, St Lucia Queensland 4067, Australia

^c Department of Agronomy, Zhejiang University, Hangzhou 310029, China

ARTICLE INFO

Article history:

Accepted 19 October 2012

Available online xxxx

Keywords:

Fusarium oxysporum

Transcriptome sequencing

Innate immune response

NADPH oxidase

Arabidopsis

ABSTRACT

We analyzed the dynamic defense transcriptome responsive to *Fusarium oxysporum* infection in *Arabidopsis* using a strand-specific RNA-sequencing approach. Following infection, 177 and 571 genes were up-regulated, 30 and 125 genes were down-regulated at 1 day-post-inoculation (1DPI) and 6DPI, respectively. Of these genes, 116 were up-regulated and seven down-regulated at both time points, suggesting that most genes up-regulated at the early stage of infection tended to be constantly up-regulated at the later stage whereas the landscape of the down-regulated genes differed significantly at the two time points investigated. In addition to genes known to be part of the defense network in various plant–pathogen interactions, many novel disease responsive genes, including non-coding RNAs, were identified. Disease inoculation experiments with mutants of the *AtROB* genes showed that *AtROBHD* and *AtROBHF* have opposite effects on disease development and provided new insights into the functions of the genes encoding NADPH oxidase in fungal disease resistance.

© 2012 Elsevier B.V. All rights reserved.

1. Introduction

Recognition of pathogens by pattern-recognition receptors (PRRs) located at the surface of plant cells activates an intricate network of signal transduction pathways leading to transcriptome reprogramming. A common mechanism for transduction of signals perceived by PRRs into cellular responses is the activation of mitogen-activated protein kinase (MAPK) cascades (Andreasson and Ellis, 2010). In *Arabidopsis*, recognition of the bacterial elicitor flg22 by the receptor kinase FLAGELLIN SENSITIVE2 (FLS2) results in rapid activation of the signaling cascade MEKK1-MKK4/MKK5-MPK3/MPK6-WRKY22/WRKY29 (Asai et al., 2002). The MKK4/MKK5-MPK3/MPK6 cascade has also recently been shown in *Botrytis cinerea*-infected *Arabidopsis* plants to regulate

biosynthesis of camalexin, a major phytoalexin in *Arabidopsis*, through transcriptional regulation of the genes involved in the camalexin biosynthesis pathway (Ren et al., 2008). Nevertheless, no MAPK cascade has been associated with defenses in response to infection with *Fusarium oxysporum*, a soil-borne plant fungal pathogen causing vascular wilt disease through roots in a wide variety of plants, including *Arabidopsis* and economically important crops such as cotton and tomato (Berrocal-Lobo and Molina, 2004).

Oxidative burst is another early defense response observed upon pathogen attack. Two major sources of pathogen-induced reactive oxygen species (ROS) are plasma membrane NADPH oxidase and cell wall peroxidase. *Arabidopsis* plants treated with Nep1 (Necrosis- and ethylene-induced peptide1), a *F. oxysporum*-derived elicitor, produce NADPH oxidase-dependent ROS, because expression of *AtRBOHD*, one of the 10 genes encoding NADPH oxidases in *Arabidopsis*, was significantly up-regulated (Bae et al., 2006). ROS production in *Arabidopsis* cell suspension cultures in response to *F. oxysporum* elicitor depends on peroxidases (Davies et al., 2006). ROS could be an important signal for both PTI and ETI (van Breusegem et al., 2008), but how *F. oxysporum*-induced ROS acts in basal resistance and in the hypersensitive response (HR) remain unclear. In other pathogen–plant interactions ROS may contribute to resistance by directly inhibiting the invading pathogen, by strengthening the host cell wall and thereby confining the pathogen in the infected site and by orchestrating HR-mediated defense gene activation (Torres et al., 2006).

Studies using mutants defective in signal transduction and defense responses have provided insights into the functions of the network

Abbreviations: MAPK or MPK, mitogen-activated protein kinase; MKK, mitogen-activated protein kinase kinase; MEKK, mitogen-activated protein kinase kinase kinase; NADPH, nicotinamide adenine dinucleotide phosphate; RBOH, respiratory burst oxidase homolog; PTI, pathogen-associated molecular pattern triggered immunity; ETI, effector-triggered immunity; qRT-PCR, quantitative reverse transcriptase PCR; AGI, the *Arabidopsis* Genome Initiative; WAK, wall-associated kinase; WAKL, wall-associated kinase like; ERF, ethylene response factor; bHLH, basic helix-loop-helix; NAC, NAM-ATAF1/2-CUC2; PTENP1, phosphatase and tensin homolog pseudogene 1; PTEN, phosphatase and tensin homolog.

* Corresponding authors.

E-mail addresses: Qianhao.Zhu@csiro.au (Q.-H. Zhu), Stuart.Stephen@csiro.au (S. Stephen), Kemal.Kazan@csiro.au (K. Kazan), Gulei.jin@zju.edu.cn (G. Jin), fanlj@zju.edu.cn (L. Fan), Jen.Taylor@csiro.au (J. Taylor), Liz.Dennis@csiro.au (E.S. Dennis), Chris.Helliwell@csiro.au (C.A. Helliwell), Ming-bo.Wang@csiro.au (M.-B. Wang).

regulating resistance to *F. oxysporum* in *Arabidopsis* (Berrocal-Lobo and Molina, 2004, 2008), but the global gene expression changes following *F. oxysporum* infection has been investigated only at a single time point (2 days-post-inoculation or 2DPI) using a microarray approach (Kidd et al., 2009, 2011), and we still know little about the dynamic defense transcriptome of *Arabidopsis* in response to *F. oxysporum* infection. Microarrays have been a reliable and cost effective tool for genome-wide gene expression analysis; however, microarrays can be used to interrogate only the annotated genes, and suffer from a lack of sensitivity due to high level of background, cross-hybridization of related sequences and signal saturation. Next-generation sequencing (NGS) technologies provide powerful alternative strategies for transcriptome analysis. RNA-sequencing, or RNA-seq, is increasingly being used for global gene expression profiling because it allows unbiased quantification of expression levels of transcripts with a higher sensitivity and broader genome coverage than microarrays (Mortazavi et al., 2008). In plants, this technology has been used to characterize the transcriptome of rice (Lu et al., 2010; Zhang et al., 2010), grapevine (Zenoni et al., 2010) and the *Arabidopsis* male meiocyte (Chen et al., 2010; Yang et al., 2011), and to identify alternative splicing events in *Arabidopsis* (Filichkin et al., 2010) and pathogen response genes in cotton (Xu et al., 2011) and soybean (Kim et al., 2011).

The goals of this study were to investigate the dynamic changes of the *Arabidopsis* defense transcriptome in response to *F. oxysporum* infection and to gain new insights about genes underlying the innate immune response against the fungal pathogen. To achieve these goals, we performed time-course transcriptome analysis using a strand-specific RNA-seq approach, which is able to distinguish the sense and antisense transcripts from the same locus and thus the expression levels of genes with antisense transcriptional activity can be estimated more accurately. The RNA-seq approach also allowed us to globally examine the expression changes of not only protein-coding genes but also non-protein coding genes that have not been included in previous microarray analyses. In addition to genes known to be responsive to pathogen infection, our study uncovered a number of novel fungal pathogen-responsive genes for further functional characterization, and provided a broader view of the dynamics of the *Arabidopsis* defense transcriptome triggered by *F. oxysporum* infection.

2. Materials and methods

2.1. Plant materials and growth conditions

Arabidopsis thaliana (ecotype Col-0) was used in all experiments. *Arabidopsis* seed was sterilized in a solution containing 33% bleach and 67% ethanol for 15 min followed by rinsing three times in 100% ethanol. Seed was then air-dried and plated on a 14-cm Petri dish containing 100 mL of Murashige-Skoog (MS) agar supplemented with 3% sucrose, and kept for 3 days at 4 °C. The Petri dish was then transferred to a growth room with a constant temperature of 22 °C and a 16 hour light/8 hour dark regime. Two-week-old seedlings were used for *F. oxysporum* infection.

2.2. Inoculation with *F. oxysporum* and disease assay

F. oxysporum (strain Fo5176, for details see Thatcher et al., 2009) was inoculated in potato dextrose broth (PDB, 1/4 strength) and grown on a shaker (28 °C) for 4 days to reach a fungal titer of $\sim 10^6$. Roots of 2-week-old seedlings were dipped in fungal spore suspension and the plants were placed on 14-cm Petri dish containing 100 mL of minimum MS agar medium without sucrose. In parallel a mock inoculation was performed by dipping roots of *Arabidopsis* seedlings in PDB (1/4 strength) and placing the plants on the minimum MS medium. Three biological replicates of whole plant sample were collected at 1 day-post-inoculation (M1DPI and F1DPI for mock and infected, respectively) and six DPI (M6DPI and F6DPI) for

RNA extraction. One replicate was used in the SOLiD RNA-seq and the other two were used in qRT-PCR confirmation.

The following *rboh* mutants obtained from the *Arabidopsis* Biological Resource Centre were used in disease inoculation experiments with *F. oxysporum*: SALK_064273 (*rbohA*), CS24635, SALK_099459 and SALK_065099 (*rbohB*), CS2259 (*rbohC*), SALK_146126 and SALK_150096 (*rbohE*), SALK_069948 and SALK_044584 (*rbohG*), SALK_058170 and SALK_136917 (*rbohH*), SALK_050665 and SALK_050658 (*rbohJ*), SALK_023622, SALK_012476 and SALK_027627 (*rbohI*). The *rbohD* and *rbohF* single mutants and the *rbohD rbohF* double mutant were previously described (Torres et al., 2002). Disease inoculation assays were done on soil grown plants of six- to eight-leaf rosette stage as previously described (Anderson et al., 2004; Kidd et al., 2009, 2011) with three replications and 20 to 40 plants used in each replication. The disease severity (percentage of leaves showing disease symptoms) and survival rates (percentage of plants that survived and set seed) were assessed 10 and 20 days post inoculations. Experiments with mutants that show altered disease resistance were independently repeated.

2.3. RNA isolation, RNA-seq library construction and sequencing

Total RNA was isolated using the RNeasy Mini Kit (Qiagen) from the *F. oxysporum*-infected (F1DPI and F6DPI) and mock-treated tissues (M1DPI and M6DPI) according to the manufacturer's instructions. The SOLiD RNA-seq libraries were created according to the procedures detailed in the SOLiD™ Whole Transcriptome Analysis Kit using 1 µg of RQ1 DNase (Promega)-treated and rRNA-depleted (two rounds of depletion using the RiboMinus™ Plant Kit, Invitrogen) total RNA and sequenced on the SOLiD™ 3 system.

2.4. Alignment of RNA-seq reads to the *Arabidopsis* reference genome and annotated genes

The *Arabidopsis thaliana* TAIR10 genome assembly and related annotations were downloaded from The *Arabidopsis* Information Resource (<http://www.arabidopsis.org/>) and a pseudo genome constructed by combining the assembly sequences with those of *F. oxysporum* (*sp lycopersici* R2) downloaded from the Fusarium Comparative Database, Broad Institute (http://www.broadinstitute.org/annotation/genome/fusarium_verticillioides/MultiHome.html). The TAIR10 annotations were complemented by including gene predictions generated by 'genaid' (release 1.3 downloaded from <http://genome.crg.es/software/genaid/>) from the TAIR10 assembly.

RNA-seq reads were aligned to the TAIR10 *Arabidopsis/Fusarium* pseudo genome using the NGS aligner Kanga (downloaded from <http://code.google.com/p/biokanga>, release 1.6.6). The *Arabidopsis/Fusarium* pseudo genome approach confers the benefit of enabling sequence reads unique to a given genome assembly to be more confidently determined where there is the possibility that some reads are not be unique to a specific genome. Alignment parameters were set to allow up to five aligner induced substitutions, microIndels up to five base pairs (bp), splice junctions up to 10000 bp, and only accepting uniquely aligned reads which are at least one Hamming from any other putative alignment. Aligned reads were filtered and only those reads exclusively aligning to the TAIR10 *Arabidopsis* assembly were retained for subsequent processing. Aligning both the mock and infected sequenced reads to an *Arabidopsis/Fusarium* pseudo genome with post-alignment filtering for *Arabidopsis* exclusive only aligned reads removes reads with sequences which by chance are homologous between *Arabidopsis* and *Fusarium* allowing for improved analysis discrimination. Retained *Arabidopsis* aligned reads were then mapped on to TAIR10 annotation loci for each individual class of annotation (protein-coding gene, pseudogene, transposon, MIRNA, snoRNA, tRNA, other RNA and genaid).

2.5. Identification of differentially expressed genes following *F. oxysporum* infection

After alignment of RNA-seq reads to the *Arabidopsis* genome, the digital expression levels (RPKM, reads per kilobase of exon model per million mapped reads; Mortazavi et al., 2008) of each annotated AGI genes were calculated. Because SOLiD RNA-seq is strand-specific, we were able to distinguish reads generated from the sense or the anti-sense strand. To more accurately estimate and compare the expression level of the annotated genes, only the reads mapped onto the sense strand of the annotated genes were used. Differentially expressed genes were identified using the NOISeq program (Tarazona et al., 2011).

2.6. Quantitative reverse transcriptase (qRT-PCR)

qRT-PCR reactions were run on the ABI PRISM™ 7900HT Fast Real-Time PCR System (ABI) using SYBR® GreenER™ qPCR SuperMix (Invitrogen). Reverse transcription was performed using 500 ng of RQ1 DNase (Promega)-treated total RNA, oligo dT and SuperScript III reverse transcriptase from the Invitrogen's First-Strand cDNA Synthesis Kit according to the manufacturer's instructions. The first-strand cDNA reaction was diluted 20 folds prior to qPCR and 5 µl of diluted cDNA was used as the PCR template. Reverse transcriptase negative controls were performed for each PCR reaction to ensure that there is no genomic DNA contamination. Ct values were determined based on two biological replicates each with two technical replicates. Relative expression levels of target genes were calculated using the $\Delta\Delta$ Ct method (Livak and Schmittgen, 2001) and with the housekeeping gene EF1 α mRNA as an internal standard. Primers used in qRT-PCR analyses were shown in Table S1.

2.7. Data access

The sequencing data have been submitted to Gene Expression Omnibus (GEO) database under the accession numbers of GSM845430–GSM845433.

3. Results and discussion

3.1. Profiling the defense transcriptome responsive to *F. oxysporum*-infection using RNA-seq

To explore the innate immune responses of *Arabidopsis* upon *F. oxysporum* infection, the transcriptome of infected plants from 1DPI (F1DPI) and 6DPI (F6DPI) was sequenced using the strand-specific SOLiD RNA-seq approach and compared with the transcriptome from mock-treated samples at the same time points (M1DPI and M6DPI). The 1DPI and 6DPI time points were chosen to capture broad disease responses of the plants and 6DPI was also the time point at which the disease symptoms (necrosis of leaf vascular tissues) could be seen. Approximately 51.6–86.2 million of raw RNA-seq reads were generated in each individual sample, and ~34.9–58.0 million of these reads were mappable (Table 1). A significant portion of the mappable reads could be aligned to multiple locations in the *Arabidopsis* genome and were excluded, and consequently, ~7.2–9.5 million of uniquely aligned reads were retained in the following analysis (Table 1).

To compare the expression levels of each annotated AGI gene model (including both protein-coding and non-protein coding) in *F. oxysporum*- and mock-treated samples, the number of RNA-seq reads uniquely mapped to the sense strand of each gene model was converted into RPKM (Mortazavi et al., 2008). To examine if RPKM could be used to measure the changes in gene expression and therefore to identify genes responsive to *F. oxysporum* infection, we performed qRT-PCR analysis for six genes with low to high expression levels (RPKM: 1–670). In general, the fold-changes of gene expression based on RPKM were highly correlated with those determined by qRT-PCR (Fig. 1). Therefore, RPKM

Table 1

Summary of RNA-seq and mapping results.

RNA-seq sample	No. of raw reads	No. of alignable reads ^a	No. of uniquely aligned reads ^a	No. of reads uniquely aligned to coding region ^b	No. of reads uniquely aligned to intergenic region ^b
M1DPI	51,632,571	34,913,661 (67.6)	7,228,458 (14.0)	5,117,871 (70.8)	716,422 (9.9)
F1DPI	52,112,724	35,984,589 (69.1)	6,809,392 (13.1)	4,824,104 (70.8)	711,406 (10.4)
M6DPI	86,192,611	57,959,792 (67.2)	9,478,132 (11.0)	6,817,880 (71.9)	988,481 (10.4)
F6DPI	58,998,007	41,385,273 (70.2)	7,981,460 (13.5)	5,652,206 (70.8)	815,449 (10.2)

^a The numbers in parentheses are the percentage of reads based on the number of raw reads.

^b The numbers in parentheses are the percentage of reads uniquely aligned to coding (not including UTR and intron) and intergenic (beyond 200 bp up- or down-stream of annotated genes) regions (based on the number of uniquely aligned reads).

was used to identify differentially expressed genes using the NOISeq program (Tarazona et al., 2011).

3.2. Identification and functional classification of genes responsive to *F. oxysporum* infection

Based on the statistics of the NOIseq approach, we found that 177 and 571 genes were up-regulated, and 30 and 125 genes down-regulated in the F1DPI and F6DPI samples, respectively (Table 2). There were more up- or down-regulated genes in F6DPI than in F1DPI, indicating a broader physiological and metabolic responses at 6DPI. Of the *F. oxysporum* responsive genes, 116 were up-regulated and seven down-regulated at both time points (Table S2). Substantial number of up- or down-regulated genes were unique to F1DPI or F6DPI, suggesting a dynamic characteristic of the defense transcriptome. In addition to protein-coding genes, a number of non-protein coding genes, including *MICRORNAs* (*MIRNAs*), pre-tRNAs and even pseudogenes, were differentially expressed upon *F. oxysporum* infection (Table 2), suggesting that they might have a role in the immune responses against the fungal pathogen or that their transcription was affected by the infection of the fungal pathogen.

A number of genes responsive to *F. oxysporum* infection identified in this study have been previously shown to be part of the defense network in various plant–pathogen interactions, for instance, genes involved in jasmonic acid (JA), indole-3-ylmethyl-glucosinolate (I3G) and camalexin biosynthesis pathways (Bednarek et al., 2009; Clay et al., 2009; Kidd et al., 2011; Pfalz et al., 2009) and disease resistance genes such as *PDF1.2* and *PR4*. Our results also confirmed the previous observation that genes involved in the biosynthesis pathways of tryptophan, I3G and camalexin are co-ordinately up-regulated in *F. oxysporum* infected *Arabidopsis* plants (Kidd et al., 2011). However, many of the *F. oxysporum* responsive genes identified here have not been previously reported, such as genes encoding dirigent-like protein (At1g64160), germin-like protein (At1g18970), CAP (Cysteine-rich secretory proteins, Antigen 5, and pathogenesis-related 1) family protein (At4g33720) and wound-responsive family proteins (At4g10270 and At4g33560).

To gain insights into the functionality of the genes responsive to *F. oxysporum* infection, we performed gene ontology (GO) term enrichment analysis (<http://bioinfo.cau.edu.cn/agriGO>) for the genes up- or down-regulated at each time point. As expected, genes related to various defense responses were significantly enriched at both time points. For the *F. oxysporum*-induced genes, the majority GO terms of biological process and molecular function and both GO terms of cellular component that were significantly enriched at 1DPI were also significantly enriched at 6DPI. In addition, many

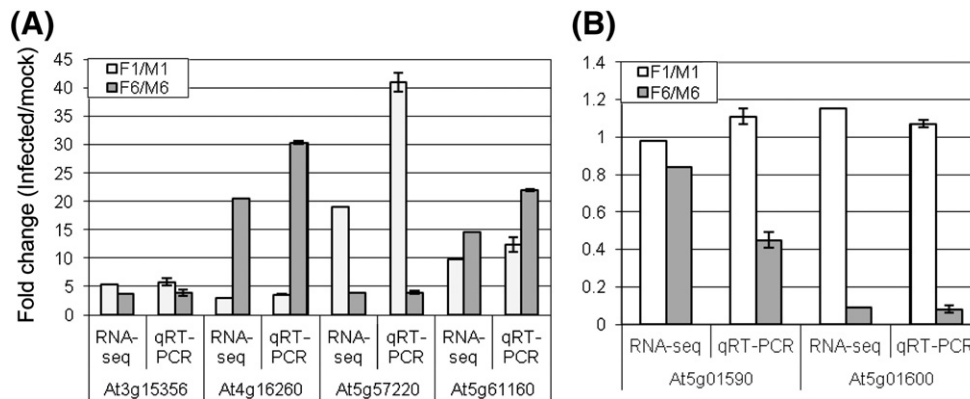


Fig. 1. qRT-PCR validation of *F. oxysporum* induced fold changes detected by RNA-seq. A, Induced genes. B, Unchanged or repressed genes. At each time point, the expression level in *F. oxysporum* infected sample was normalized to that in its corresponding mock sample. Standard error bars for the fold changes determined by qRT-PCR are shown.

more GO terms were significantly enriched at 6DPI (Table S3). This suggests that the defense responses initiated at the early stage of fungal pathogen infection continued to play a role at the later stage although many more defense responses were further induced at the later stage. In terms of hormone responses, at 1DPI only genes responsive to ethylene (ET)-stimulus were enriched, but at 6DPI other hormone responsive genes were also enriched. These include genes involved in JA metabolism and signaling, genes involved in tryptophan metabolism that leads to auxin biosynthesis, and genes responsive to salicylic acid (SA) and abscisic acid (ABA) stimulus and involved in the regulation of systemic acquired resistance (SAR) (Table S3). These results indicate that the ET, JA, auxin and SA pathways are all activated in response to infection of *F. oxysporum* but act at different times. The ET signaling pathway appears to be activated earlier than the pathways related to signaling of other hormones.

The *F. oxysporum*-repressed genes were significantly different at 1DPI and 6DPI. The impact of *F. oxysporum* infection on root development was evident at 1DPI as genes related to root epidermal cell differentiation and root system development were down-regulated (Table S3). This observation is consistent with previous results from plants treated with Nep1 (Bae et al., 2006). Probably because of impaired root development and cell wall disorganization, the growth of the infected plants became slower, their ability to respond to light stimulus was reduced and their photosynthesis was significantly impaired at 6DPI as evidenced by the down-regulation of genes encoding the components of the light harvesting complex (Table S3).

3.3. Novel genes involved in the defense network responsive to *F. oxysporum* infection

To search for novel genes involved in recognition of fungal pathogen, signal transduction and disease resistance, we checked the expression

Table 2
Classification of *Arabidopsis* genes responsive to *Fusarium oxysporum* infection.

Gene type	1DPI		6DPI	
	Induced ^a	Repressed ^a	Induced ^a	Repressed ^a
Protein coding	172 (115)	18 (7)	549 (115)	117 (7)
MIRNA	1	2	8	0
Other RNA	0	1	1	0
Pre-tRNA	3	9	8	7
Pseudogene	1 (1)	0	5 (1)	1
Total	177	30	571	125

^a The numbers in parentheses indicate the number of genes co-induced or co-repressed at both time points.

dynamics of these types of genes as well as genes encoding transcription factors (TFs) in the *F. oxysporum*-infected and mock-treated samples.

Among the *WAK/WAKL* family genes, the highest induction upon *F. oxysporum* infection was observed for *WAK1*, *WAK3* and *WAKL10* (Table 3). Previous studies have shown that *WAK1* is induced by the fungal pathogen *Alternaria brassicicola* (Schenk et al., 2000) and up-regulation of *WAK1* is required for SAR (Maleck et al., 2000). However, the functions of *WAK3* and *WAKL10* have not yet been reported. Among genes encoding putative receptors or receptor-like kinases (RLKs), At3g59700, At5g01540 and At5g60900 were consistently induced at both time points, At1g65790 and At4g13920 were mainly induced in 6DPI (Table 3). The induction of a number of RLKs by *F. oxysporum* infection could be due to the requirement of recognition of multiple elicitors released by *F. oxysporum*. Like PRR activation, down-regulation of PRR signaling is also crucial. It prevents excessive or prolonged activation of immune responses that would be detrimental to the host. A recent study discovered that two closely related plant U-box ubiquitin ligases, PUB12 and PUB13, were induced by flg22 and recruited to the FLS2 receptor complex resulting in enhanced polyubiquitination and degradation of FLS2 (Lu et al., 2011). These U-box genes also contain a C-terminal ARMADILLO (ARM) repeat domain. Our data showed that at least one plant U-box gene (*PUB23*) and a couple of ARM repeat domain-containing genes were significantly up-regulated at both time points (Table 3), suggesting that *F. oxysporum*-induced immune responses may also require down-regulation of PRR signals.

Arabidopsis RIN4 (RPM1-interacting protein 4) is a well-studied negative regulator of plant immunity. Phosphorylation and proteolytic cleavage of RIN4 by bacterial effectors activates RIN4-associated resistance (R) proteins RPM1 (Resistance to *Pseudomonas syringae* pv *maculicola* 1) and RPS2 (resistance to *P. syringae* 2), respectively, which results in rapid initiation of ETI and defense signaling and restricts further colonization of pathogen (Liu et al., 2009). Our results showed that the expression levels of *RIN4*, *RPM1* and *RPS2* were not affected by *F. oxysporum* infection at any time point (data not shown), but At3g48450, a RIN4 family gene was induced 10.3 and 12.2 folds in 1DPI and 6DPI, respectively. Furthermore, two genes associated with RIN4 (Liu et al., 2009), At3g28220 encoding a MATH domain-containing protein and At1g52000 encoding a lectin, were induced 12.5 and 6.0 folds in 6DPI, respectively. This result suggests a potential role of these genes in plant defense against *F. oxysporum*. Several TIR (Toll interleukin 1 receptor)-class R genes that have not been previously reported were also induced following *F. oxysporum* infection (Table 3).

The cytochrome P450 genes involved in JA, indole glucosinolate, camalexin and callose biosynthesis pathways were all highly induced in the *F. oxysporum* infected plants, consistent with the published results (Bednarek et al., 2009; Clay et al., 2009; Kidd et al., 2011; Liu et al., 2010).

Table 3Novel genes responsive to *Fusarium oxysporum* infection.

AGI ID	Gene name or description	Expression level (RPKM) and fold change					
		M1DPI	F1DPI	F1/M1 ^a	M6DPI	F6DPI	F6/M6 ^a
AT1G21250	WAK1	29.48	45.60	1.55	18.03	92.09	5.11*
AT1G21240	WAK3	3.11	5.88	1.89	0.82	17.24	21.03*
AT1G79680	WAKL10	0.31	2.44	7.79*	1.00	10.05	10.05*
AT1G65790	Receptor kinase 1	2.10	3.23	1.54	0.72	6.00	8.32*
AT3G59700	Lectin-receptor kinase	1.49	4.48	3.01*	1.90	8.27	4.36*
AT4G13920	Receptor like protein 50	1.25	2.56	2.04	0.77	8.42	10.89*
AT5G01540	Lectin receptor kinase a4.1	1.33	3.74	2.80*	1.18	6.19	5.24*
AT5G60900	Receptor-like protein kinase 1	2.78	5.84	2.10*	0.99	7.88	7.93*
AT2G35930	Plant U-box 23	5.50	16.13	2.93*	9.10	21.29	2.34*
AT3G02840	ARM repeat superfamily protein	0.52	6.08	11.68*	4.85	12.55	2.59*
AT5G09800	ARM repeat superfamily protein	1.52	4.03	2.65	1.16	5.55	4.79*
AT5G67340	ARM repeat superfamily protein	0.82	5.97	3.28*	1.43	9.83	6.86*
AT1G57630	TIR class	1.79	9.25	5.16*	1.96	16.60	8.49*
AT3G04220	TIR-NBS-LRR class	0.41	2.17	5.31*	0.62	5.06	8.10*
AT4G11170	TIR-NBS-LRR class	0.20	4.29	21.23*	0.34	5.90	17.36*
AT1G64160	Ddirigent-like	0.16	21.26	132.70*	3.67	55.38	15.09*
AT4G19230	CYP707A1	3.60	13.03	3.62*	3.16	28.41	8.99*
AT2G24180	CYP71B6	21.03	77.60	3.69*	19.70	95.56	4.85*
AT4G31950	CYP82C3	0.08	2.43	30.38	0.13	5.57	42.85*
AT4G37430	CYP91A2	1.21	1.68	1.39	0.92	8.21	8.91*
AT5G52320	CYP96A4	2.65	4.55	1.72	2.44	14.25	5.84*
AT5G64810	WRKY51	2.46	15.66	6.37*	2.17	14.98	6.91*
AT3G01970	WRKY45	5.53	25.80	4.67*	13.78	76.35	5.54*
AT1G66600	WRKY63	0.47	4.03	8.49*	1.21	9.39	7.78*
AT5G13080	WRKY75	4.22	19.40	4.60*	10.60	43.48	4.10*
AT3G23250	MYB15	0.69	12.61	18.20*	6.65	21.39	3.21*
AT1G48000	MYB112	0.88	1.87	2.12	0.11	8.20	73.08*
AT1G66370	MYB113	0	0		0	11.47	*
AT2G31230	ATERF15/ERF#093	3.01	7.04	2.34	2.19	27.11	12.41*
AT3G56970	AtbHLH038	9.62	44.43	4.62*	0.78	90.69	116.35*
AT3G56980	AtbHLH039	11.20	39.02	3.48*	3.01	58.50	19.42*
AT5G04150	AtbHLH101	17.84	28.12	1.58	0.42	30.13	71.50*
AT4G34590	AtbZIP11,ATB2	3.30	5.26	1.59	2.08	11.71	5.64*
AT5G49300	GATA-16	3.11	4.62	1.49	0.63	6.15	9.72*
AT1G02220	ANAC003	6.49	23.06	3.55*	4.58	34.32	7.50*
AT2G43000	ANAC042	1.21	18.09	15.00*	1.38	12.89	9.33*
AT3G10040	Sequence-specific DNA binding transcription factor	1.93	13.97	7.25*	2.45	14.95	6.10*

^a *Indicates significantly induced.

CYP76C2, activated by bacteria *P. syringae* carrying avirulence genes (Godiard et al., 1998), was also induced by *F. oxysporum* infection, particularly in F6DPI. In addition, we found that a few other uncharacterized cytochrome P450 genes were also highly induced in F6DPI or at both time points (Table 3), implying a role of these P450 genes in response to *F. oxysporum* infection. One of these was CYP82C3, a homolog of CYP82C2 that affects JA-induced accumulation of the indole glucosinolate biosynthetic precursor tryptophan (Liu et al., 2010).

Defense-associated genes are normally regulated positively or negatively by transcription factors that are direct or indirect targets of various signal transduction pathways. Of the ~1400 TFs according to Czechowski et al. (2004), 12 were significantly induced in F1DPI and 10 of these TFs (MYB122; ANAC03, 42; AtbHLH038, 039; WRKY45, 51, 53, 63, 75) (Table 3; Table S2) were also significantly induced in F6DPI. Of these constantly induced TFs, only MYB122 and WRKY53 have been functionally characterized. WRKY53 is a positive regulator of defense responses against virulent bacteria *P. syringae* (Wang et al., 2006). Overexpression of MYB122 causes a high-auxin phenotype and increases levels of indolic glucosinolates in *Arabidopsis* plants (Gigolashvili et al., 2007). The two TFs uniquely induced in F1DPI were MYB15 and MYB51. MYB51 and MYB122 are homologs, and activation of MYB51 leads to increased activity of indolic glucosinolate biosynthetic genes and consequently accumulation of indolic glucosinolates; however, *Arabidopsis* plants overexpressing MYB51 did not show alternated auxin metabolism as seen in plants overexpressing MYB122 (Gigolashvili et al., 2007), suggesting that MYB51 has a unique role in regulating biosynthesis of antimicrobial substance. The TFs uniquely induced in F6DPI include ERF1 (At3g23240) and

ANAC019 (At1g52890). *Arabidopsis* plants overexpressing ERF1 were more resistant to *F. oxysporum*, which is thought to be achieved through ET-mediated pathway (Berrocal-Lobo and Molina, 2004). ANAC019 has been shown to act down-stream of MYC2 to regulate JA-signaled defense response (Bu et al., 2008). No significantly repressed TF was found in F1DPI but seven TFs were significantly repressed in F6DPI and none of them has been functionally characterized. These results indicate that different TFs are dynamically activated or repressed at the early or later time point following *F. oxysporum* infection although some TFs were constitutively up-regulated at both time points. The majority of these *F. oxysporum*-responsive TFs belong to the WRKY, ERF, MYB, bHLH and NAC families (Table 3).

3.4. Diverse roles of *AtROBH* genes in response to *F. oxysporum* infection

Our results indicate that oxidative burst is one of the earliest defense responses observed upon *F. oxysporum* infection (Table S2). In *Arabidopsis* a 10-member gene family (*AtROBHA*–*AtROBHJ*) encodes homologues of the mammalian NADPH oxidase gp91phox (Torres and Dangel, 2005). *AtROBHD* and *AtROBHF* have been shown to be required for the production of a full oxidative burst in response to avirulent strains of the bacterial pathogen *P. syringae* and the oomycete *Hyaloperonospora parasitica*, respectively (Torres et al., 2002). Our RNA-seq analysis results showed that the highest basal expression levels of the 10 *AtROBH* genes were observed for *AtROBHD*. The expression levels of *AtROBHA*, *AtROBHB*, *AtROBHD* and *AtROBHF* were increased at both time points following *F. oxysporum* infection;

however, a significant induction was only observed for *AtROBHD* (in both F1DPI and F6DPI) and *AtROBHF* (in F6DPI) (Fig. 2a).

To determine whether members of the *AtROBH* gene family affect resistance to *F. oxysporum*, we have conducted extensive disease inoculation experiments with mutant lines of this gene family (see **Materials and methods**). Of the mutant lines tested, a significantly altered disease phenotype could only be observed for *rbohD*, *rbohF* and *rbohD rbohF* double mutant (Figs. 2b–d). The *rbohD* and *rbohF* mutants displayed significantly increased and reduced disease resistance, respectively. These results suggest that these two NADPH oxidase encoding genes have opposing effects on disease development. Confirming this result, the *rbohD rbohF* mutant showed an intermediate disease phenotype that was somewhat similar to that observed in wild type plants. Previous research has indicated that RBOHD and RBOHF can indeed have diverse roles in plant–pathogen interactions, hormone signaling and cell death. For instance, it was demonstrated that RBOHD antagonizes cell death triggered by SA and SA analog benzothiadiazole (BTH) in the *Arabidopsis lsd1* mutant (Torres et al., 2005). However, a similar role for RBOHF in negative regulation of cell death is not known. In addition a role for RBOHD in systemic (root to shoot) signaling mediated by diverse stimuli has been shown (Miller et al., 2009). It is, therefore, possible that ROS- and pathogen-induced senescence responses that are implicated in promoting disease symptom development (Thatcher et al., 2009) are attenuated in the *rbohD* mutant. Another

reason for the increased disease phenotype of the *rbohD* mutant could be due to increased levels of SA accumulation following pathogen inoculation (Pogány et al., 2009), which is known to be required for resistance to this pathogen (Edgar et al., 2006). Similar to our results with the *rbohF* mutant showing increased disease susceptibility, the inhibition of the expression of the barley (*Hordeum vulgare* L.) homolog of the *Arabidopsis* RBOHF also shows increased susceptibility to the powdery mildew pathogen *Blumeria graminis* f. sp. *hordei* (Proels et al., 2010). Although the exact reason(s) why these two ROS-producing genes differentially affect *F. oxysporum* resistance require additional investigation, results from inoculation experiments show that the genes identified through RNA-seq analysis have relevance to this interaction.

3.5. *F. oxysporum* responsive non-protein coding RNAs

miRNAs (microRNAs) have been implicated in various biotic and abiotic stress responses (Sunkar, 2010), and several miRNAs have recently been shown to positively or negatively regulate flg22-induced callose deposition in *Arabidopsis* (Li et al., 2010). MIRNAs, particularly the conserved MIRNAs, usually contain multiple members that generate the same mature miRNA; therefore it is often difficult to evaluate the relative importance of individual MIRNA family members based on small RNA sequencing unless different family members have a different miRNA passenger strand (miRNA*) sequence. RNA-seq is now enabling

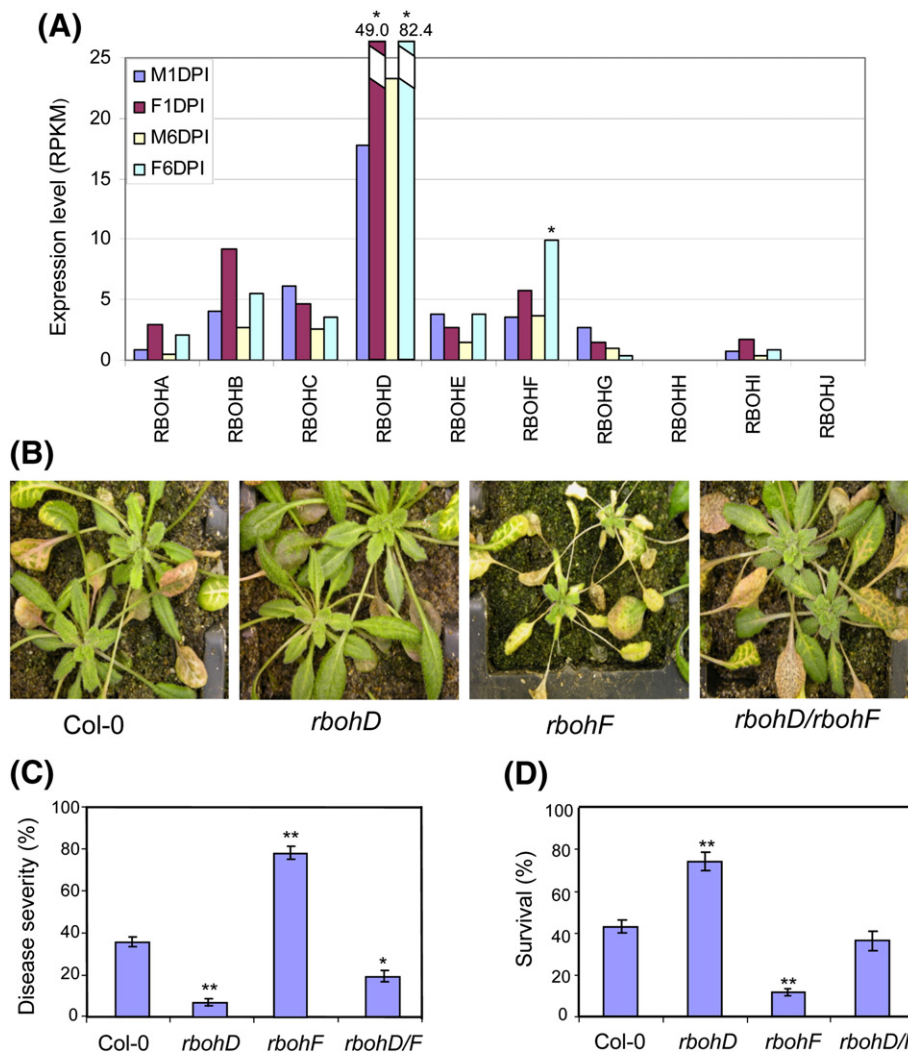


Fig. 2. Analysis of the genes encoding NADPH oxidase. A, Expression profile of genes encoding NADPH oxidases. B, Phenotypic changes observed in *rbohD*, *rbohF* single mutant and *rbohD rbohF* double mutant. C, The disease severity (percentage of leaves showing disease symptoms). D, The survival rates (percentage of plants that survived and set seed). The disease severity and the survival rates were assessed 10 and 20 days after inoculations. * and ** refer to significant differences at $p < 0.05$ and 0.01 , respectively.

Table 4
MIRNA genes responsive to *Fusarium oxysporum* infection.

AGI ID	MIRNA and target ^a	Expression level (RPKM) and fold change					
		M1DPI	F1DPI	F1/M1 ^b	M6DPI	F6DPI	F6/M6 ^b
AT3G10745	MIR158a	2.66	4.24	1.59	3.05	17.95	5.89*
AT2G03220	AtFUT1	7.95	6.18	0.78	5.64	6.45	1.14
AT1G18075	MIR159b	0.71	2.28	3.18	0.55	6.44	11.79*
AT5G06100	MYB33	4.96	8.15	1.64	6.34	13.01	2.05
AT3G11440	MYB65	3.89	5.39	1.39	4.13	8.20	1.98
AT5G46845	MIR160c	4.93	0	*	2.51	2.96	1.18
AT2G28350	ARF10	6.34	4.74	0.75	4.41	7.71	1.75
AT4G30080	ARF16	6.93	6.34	0.91	7.06	10.90	1.54
AT5G23065	MIR162b	1.51	3.21	2.12	0.00	9.52	*
AT1G01040	DCL1	12.60	11.20	0.89	11.80	16.50	1.40
AT3G61897	MIR166b	13.06	2.52	0.19*	10.88	6.41	0.59
AT5G41905	MIR166e	3.94	4.18	1.06	0.00	5.32	*
AT1G30490	ATHB9	5.80	5.43	0.94	7.96	13.00	1.63
AT1G52150	ATHB15	13.02	13.90	1.07	11.54	14.16	1.23
AT2G34710	ATHB14	6.94	7.97	1.15	6.30	5.66	0.90
AT4G32880	ATHB8	9.24	8.73	0.95	8.00	8.43	1.05
AT5G14545	MIR398b	16.05	23.12	1.44	21.89	57.78	2.64*
AT5G14565	MIR398c	6.10	8.95	1.47	7.12	22.94	3.22*
AT1G08830	CSD1	84.00	109.00	1.30	69.80	41.40	0.59
AT2G28190	CSD2	33.00	15.90	0.48	22.50	8.54	0.38*
AT1G12520	CCS1	20.10	18.00	0.90	16.60	10.00	0.60
AT2G47015	MIR408	1.92	2.04	1.06	3.42	9.41	2.75*
AT2G02850	ARPN	7.33	10.40	1.42	3.87	4.90	1.27
AT2G30210	LAC3	7.46	5.24	0.70	3.52	2.16	0.61
AT5G07130	LAC13	1.69	1.56	0.92	1.63	1.39	0.85
AT4G32445	MIR419	1.25	6.66	5.33*	1.92	2.26	1.18

^a Only confirmed targets are shown.

^b *Indicates significantly induced or repressed.

us to solve this problem by examining the accumulation level of the corresponding primary or precursor miRNA transcripts (pri- or pre-miRNAs) that often have distinct sequences for individual members of a MIRNA family.

In the *Arabidopsis* TAIR10 assembly, 338 members of 194 MIRNA families have been annotated (miRBase V18). Using a RPKM threshold of ≥ 1 in at least one sample, we detected the expression of 84 pre-miRNAs or pri-miRNAs of 56 MIRNA families, representing 25% of the total MIRNA genes. Generally, the RPKM value (0–58) was low for the majority of MIRNAs, suggesting that MIRNAs are either expressed at low levels or rapidly processed. The expression levels of the majority of the detected MIRNAs were not affected by *F. oxysporum* infection, but 10 MIRNAs, belonging to eight families, were up- or down-regulated at the different time points (Table 4).

Up-regulation of pri- or pre-miRNA transcripts triggered by *F. oxysporum* infection could result from increased transcription of a MIRNA gene or decreased processing of pri- or pre-miRNA. Similarly, reduced accumulation of MIRNA transcripts following *F. oxysporum* infection could be due to decreased transcription of the MIRNA gene or increased processing of pri- or pre-miRNA. These two possible mechanisms could be partly distinguished based on the expression level of the miRNA target genes although this could be complicated by the presence of multiple members in a MIRNA family and the possible existence of miRNA-mediated translational repression in addition to miRNA-mediated mRNA cleavage. In most cases, up- or down-regulation of MIRNA following *F. oxysporum* infection did not lead to changes in the expression levels of their targets. In the case of MIR159b, the expression levels of its target genes MYB33 and MYB65 were slightly induced rather than repressed (Table 4). These results could imply that *F. oxysporum* infection generally inhibits the processing of pri- or pre-miRNAs although this needs further experimental confirmation. However, the enhanced expression of MIR398b and MIR398c in F6DPI was correlated with the down-regulation of their target genes, particularly Copper superoxide dismutase2 (CSD2; Table 4), suggesting that the miR398-mediated regulation of CSD genes might be part of the defense network against *F. oxysporum* infection in *Arabidopsis*. A recent study

showed that a number of miRNAs, particularly those targeting genes that are involved in plant hormone biosynthesis and signaling pathways, were differentially expressed in *Arabidopsis* in response to infection of bacterial pathogen *P. syringae* pv. *tomato* (Zhang et al., 2011).

We found that the expression levels of several pseudogenes were significantly changed following *F. oxysporum* infection (Table 2). One of these pseudogenes, At2g16367 annotated as similar to defensin-like gene, was induced by 6.8 and 8.3 folds in F1DPI and F6DPI, respectively; whereas five pseudogenes were specifically induced in F6DPI. Recent studies in animal and human indicate that transcripts generated from pseudogenes are able to regulate the activity of protein-coding genes through their ability to compete for miRNA binding, thereby protecting miRNA target RNAs from repression. For example, the human pseudogene PTENP1, which is related to the tumor suppressor gene PTEN, is transcribed to produce a non-protein RNA. Because both PTEN and PTENP1 contain many conserved miRNA binding sites in their 3' untranslated regions (UTRs), PTENP1 was found to regulate the expression of PTEN by acting as a decoy for miRNAs that bind to the common sites in the 3' UTRs of PTENP1 and PTEN (Tay et al., 2011). Whether the *F. oxysporum*-responsive pseudogenes play a role in resistance to fungal pathogen, and if so, whether they function like PTENP1 or using other yet to be uncovered mechanism are still open questions.

4. Conclusions

The time-course RNA-seq analysis results showed that 1) upon *F. oxysporum* infection, the biogenesis and signaling pathways of ET, SA and JA were co-ordinately activated with the ET-mediated signaling pathway activated earlier than the JA- and SA-mediated signaling pathways; 2) a number of different types of receptor-like protein kinases and putative R genes were specifically induced at different time points, suggesting a distinct role of these genes at specific stage(s) following *F. oxysporum* infection; 3) in addition to TFs with known function in response to pathogen attack, novel *F. oxysporum* responsive TFs were identified, and TFs induced at 1DPI tend to be induced at 6DPI as well; 4) several MIRNAs and pseudogenes were found to be differentially expressed following *F. oxysporum* infection. In addition, RNA-seq and disease inoculation experiments discovered that of the 10 ROBH genes in *Arabidopsis*, only AtROBHD and AtROBHF were *F. oxysporum* responsive and they had an opposite effect on disease development.

Supplementary data to this article can be found online at <http://dx.doi.org/10.1016/j.gene.2012.10.036>.

Acknowledgments

This study was supported by the CSIRO Transformational Biology Capability Platform. Authors are grateful to Dr Frank Gubler for helpful discussions.

References

- Anderson, J.P., et al., 2004. Antagonistic interaction between abscisic acid and jasmonate-ethylene signaling pathways modulates defense gene expression and disease resistance in *Arabidopsis*. *Plant Cell* 16, 3460–3479.
- Andreasson, E., Ellis, B., 2010. Convergence and specificity in the *Arabidopsis* MAPK nexus. *Trends Plant Sci.* 15, 106–113.
- Asai, T., et al., 2002. MAP kinase signaling cascade in *Arabidopsis* innate immunity. *Nature* 415, 977–983.
- Bae, H., Kim, M.S., Sicher, R.C., Bae, H.J., Bailey, B.A., 2006. Necrosis- and ethylene-inducing peptide from *Fusarium oxysporum* induces a complex cascade of transcripts associated with signal transduction and cell death in *Arabidopsis*. *Plant Physiol.* 141, 1056–1067.
- Bednarek, P., et al., 2009. A glucosinolate metabolism pathway in living plant cells mediates broad-spectrum antifungal defense. *Science* 323, 101–106.
- Berrocal-Lobo, M., Molina, A., 2004. Ethylene response factor 1 mediates *Arabidopsis* resistance to the soilborne fungus *Fusarium oxysporum*. *Mol. Plant Microbe Interact.* 17, 763–770.
- Berrocal-Lobo, M., Molina, A., 2008. *Arabidopsis* defense response against *Fusarium oxysporum*. *Trends Plant Sci.* 13, 145–150.

- Bu, Q., et al., 2008. Role of the *Arabidopsis thaliana* NAC transcription factors ANAC019 and ANAC055 in regulating jasmonic acid-signaled defense responses. *Cell Res.* 18, 756–767.
- Chen, C., et al., 2010. Meiosis-specific gene discovery in plants: RNA-Seq applied to isolated *Arabidopsis* male meiocytes. *BMC Plant Biol.* 10, 280.
- Clay, N.K., Adio, A.M., Denoux, C., Jander, G., Ausubel, F.M., 2009. Glucosinolate metabolites required for an *Arabidopsis* innate immune response. *Science* 323, 95–101.
- Czechowski, T., Bari, R.P., Stitt, M., Scheible, W., Udvardi, M.K., 2004. Real-time RT-PCR profiling of over 1400 *Arabidopsis* transcription factors: unprecedented sensitivity reveals novel root- and shoot-specific gene. *Plant J.* 38, 366–379.
- Davies, D.R., Bindschedler, L.V., Strickland, T.S., Bolwell, G.P., 2006. Production of reactive oxygen species in *Arabidopsis thaliana* cell suspension cultures in response to an elicitor from *Fusarium oxysporum*: implications for basal resistance. *J. Exp. Bot.* 57, 1817–1827.
- Edgar, C.I., et al., 2006. Salicylic acid mediates resistance to the vascular wilt pathogen *Fusarium oxysporum* in the model host *Arabidopsis thaliana*. *Aust. Plant Pathol.* 35, 581–591.
- Filichkin, S.A., et al., 2010. Genome-wide mapping of alternative splicing in *Arabidopsis thaliana*. *Genome Res.* 20, 45–58.
- Gigolashvili, T., Berger, B., Mock, H.P., Müller, C., Weisshaar, B., Flügge, U.I., 2007. The transcription factor HIG1/MYB51 regulates indolic glucosinolate biosynthesis in *Arabidopsis thaliana*. *Plant J.* 50, 886–901.
- Godiard, L., et al., 1998. CYP76C2, an *Arabidopsis thaliana* cytochrome P450 gene expressed during hypersensitive and developmental cell death. *FEBS Lett.* 438, 245–249.
- Kidd, B.N., et al., 2009. The Mediator complex subunit PFT1 is a key regulator of jasmonate-dependent defense in *Arabidopsis*. *Plant Cell* 21, 2237–2252.
- Kidd, B.N., et al., 2011. Auxin signaling and transport promote susceptibility to the root-infecting fungal pathogen *Fusarium oxysporum* in *Arabidopsis*. *Mol. Plant Microbe Interact.* 24, 733–748.
- Kim, K.H., et al., 2011. RNA-Seq analysis of a soybean near-isogenic line carrying bacterial leaf pustule-resistant and -susceptible alleles. *DNA Res.* 18, 483–497.
- Li, Y., Zhang, Q., Zhang, J., Wu, L., Qi, Y., Zhou, J.M., 2010. Identification of microRNAs involved in pathogen-associated molecular pattern-triggered plant innate immunity. *Plant Physiol.* 152, 2222–2231.
- Liu, J., Elmore, J.M., Coaker, G., 2009. Investigating the functions of the RIN4 protein complex during plant innate immune responses. *Plant Signal. Behav.* 4, 1107–1110.
- Liu, F., et al., 2010. The *Arabidopsis* P450 protein CYP82C2 modulates jasmonate-induced root growth inhibition, defense gene expression and indole glucosinolate biosynthesis. *Cell Res.* 20, 539–552.
- Livak, K.J., Schmittgen, T.D., 2001. Analysis of relative gene expression data using real-time quantitative PCR and the $2^{-\Delta\Delta Ct}$ method. *Methods* 25, 402–408.
- Lu, T., et al., 2010. Function annotation of the rice transcriptome at single-nucleotide resolution by RNA-seq. *Genome Res.* 20, 1238–1249.
- Lu, D., et al., 2011. Direct ubiquitination of pattern recognition receptor FLS2 attenuates plant innate immunity. *Science* 332, 1439–1442.
- Maleck, K., et al., 2000. The transcriptome of *Arabidopsis thaliana* during systemic acquired resistance. *Nat. Genet.* 26, 403–410.
- Miller, G., et al., 2009. The plant NADPH oxidase RBOHD mediates rapid systemic signaling in response to diverse stimuli. *Sci. Signal.* 2, ra45.
- Mortazavi, A., Williams, B.A., McCue, K., Schaeffer, L., Wold, B., 2008. Mapping and quantifying mammalian transcriptomes by RNA-Seq. *Nat. Methods* 5, 621–628.
- Pfalz, M., Vogel, H., Kroymann, J., 2009. The gene controlling the indole glucosinolate modifier1 quantitative trait locus alters indole glucosinolate structures and aphid resistance in *Arabidopsis*. *Plant Cell* 21, 985–999.
- Pogány, M., et al., 2009. Dual roles of reactive oxygen species and NADPH oxidase RBOHD in an *Arabidopsis-Alternaria* pathosystem. *Plant Physiol.* 151, 1459–1475.
- Proels, R.K., Oberhollenzer, K., Pathuri, I.P., Hensel, G., Kumlehn, J., Hükelhoven, R., 2010. RBOHF2 of barley is required for normal development of penetration resistance to the parasitic fungus *Blumeria graminis* f. sp. *Hordei*. *Mol. Plant Microbe Interact.* 23, 1143–1150.
- Ren, D., et al., 2008. A fungal-responsive MAPK cascade regulates phytoalexin biosynthesis in *Arabidopsis*. *Proc. Natl. Acad. Sci. U. S. A.* 105, 5638–5643.
- Schenk, P.M., et al., 2000. Coordinated plant defense responses in *Arabidopsis* revealed by microarray analysis. *Proc. Natl. Acad. Sci. U. S. A.* 97, 11655–11660.
- Sunkar, R., 2010. MicroRNAs with macro-effects on plant stress responses. *Semin. Cell Dev. Biol.* 21, 805–811.
- Tarazona, S., García-Alcalde, F., Dopazo, J., Ferrer, A., Conesa, A., 2011. Differential expression in RNA-seq: a matter of depth. *Genome Res.* 21, 2213–2223.
- Tay, Y., et al., 2011. Coding-independent regulation of the tumor suppressor PTEN by competing endogenous mRNAs. *Cell* 147, 344–357.
- Thatcher, L.F., Manners, J.M., Kazan, K., 2009. *Fusarium oxysporum* hijacks COI1-mediated jasmonate signaling to promote disease development in *Arabidopsis*. *Plant J.* 58, 927–939.
- Torres, M.A., Dangl, J.L., 2005. Functions of the respiratory burst oxidase in biotic interactions, abiotic stress and development. *Curr. Opin. Plant Biol.* 8, 397–403.
- Torres, M.A., Dangl, J.L., Jones, J.D., 2002. *Arabidopsis* gp91phox homologues AtrbohD and AtrbohF are required for accumulation of reactive oxygen intermediates in the plant defense response. *Proc. Natl. Acad. Sci. U. S. A.* 99, 517–522.
- Torres, M.A., Jones, J.D., Dangl, J.L., 2005. Pathogen-induced, NADPH oxidase-derived reactive oxygen intermediates suppress spread of cell death in *Arabidopsis thaliana*. *Nat. Genet.* 37, 1130–1134.
- Torres, M.A., Jones, J.D., Dangl, J.L., 2006. Reactive oxygen species signaling in response to pathogens. *Plant Physiol.* 141, 373–378.
- van Breusegem, F., Bailey-Serres, J., Mittler, R., 2008. Unraveling the tapestry of networks involving reactive oxygen species in plants. *Plant Physiol.* 147, 978–984.
- Wang, D., Amornsiripanitch, N., Dong, X., 2006. A genomic approach to identify regulatory nodes in the transcriptional network of systemic acquired resistance in plants. *PLoS Pathog.* 2, e123.
- Xu, L., et al., 2011. Lignin metabolism has a central role in the resistance of cotton to the wilt fungus *Verticillium dahliae* as revealed by RNA-Seq-dependent transcriptional analysis and histochemistry. *J. Exp. Bot.* 62, 5607–5621.
- Yang, H., Lu, P., Wang, Y., Ma, H., 2011. The transcriptome landscape of *Arabidopsis* male meiocytes from high-throughput sequencing: the complexity and evolution of the meiotic process. *Plant J.* 65, 503–516.
- Zenoni, S., et al., 2010. Characterization of transcriptional complexity during berry development in *Vitis vinifera* using RNA-Seq. *Plant Physiol.* 152, 1787–1795.
- Zhang, G., et al., 2010. Deep RNA sequencing at single base-pair resolution reveals high complexity of the rice transcriptome. *Genome Res.* 20, 646–654.
- Zhang, W., et al., 2011. Bacteria-responsive microRNAs regulate plant innate immunity by modulating plant hormone networks. *Plant Mol. Biol.* 75, 93–105.